

High precipitation rates increase potassium density in plant communities in the Tibetan Plateau

Xin Li^{1,2}, Mingxu Li¹✉, Xiaoyu Cen^{1,2}, Li Xu¹ & Nianpeng He^{1,2,3}✉

Potassium is essential for plant growth. However, our understanding of potassium in plant materials is limited due to a lack of systematic studies. Here, we measured potassium content in 2,040 ecosystem communities during the period 2019–2021 applying grid-sampling and explored the spatial patterns and drivers of potassium density in the Tibetan Plateau vegetation. Potassium content, density, and storage were estimated at 8.63 milligrams per grams, 21.71 grams per square meter, and 19.92 teragrams, respectively. Potassium allocation was isometric in most ecosystems, except for deserts which followed optimal partitioning. Precipitation was the main driver of potassium variations, with higher potassium in humid regions. The spatial distribution, as revealed by random forests model, indicated higher potassium in the southeastern regions but lower potassium values in the northwestern regions. Our research sheds light on climate change's impact on vegetation potassium, offering valuable data for biogeochemical cycle optimization.

¹Key Laboratory of Ecosystem Network Observation and Modeling, Institute of Geographic Sciences and Natural Resources Research, Chinese Academy of Sciences, 100101 Beijing, China. ²College of Resources and Environment, University of Chinese Academy of Sciences, 100049 Beijing, China. ³Center for Ecological Research, Northeast Forestry University, 150040 Harbin, China. ✉email: mingxuli@igsrr.ac.cn; hemp@igsrr.ac.cn

Plant growth is inseparable from nutrient elements in nature, plants commonly experience stress from the lack of many of these nutrient elements¹, especially potassium (K). Lucanus² first recognized the vital role of K as an essential element for plant growth. K is the most abundant metal ion in plants, playing a crucial role in absorption, stomatal movement, enzyme activation, and protein synthesis³. Despite its importance, a substantial global soil deficiency persists, affecting up to 50% of soils in agricultural areas^{4,5}. This exacerbates the conflict between soil K deficiency and sustainable plant productivity⁶.

The Tibetan Plateau (TP) has garnered significant attention in scientific research since its initial characterization by Lóczy⁷. The TP presents an exceptional and advantageous avenue for research owing to its heterogeneous plant communities, extensive spectrum of humidity, temperature and radiation gradients, and trifling anthropogenic influence. Thus, the TP provides a unique opportunity to examine vegetation–environment interrelationships⁸. Despite its potential, studies in terrestrial ecosystems have predominantly focused on nitrogen (N) and phosphorus (P), which are the main components of proteins and nucleic acids⁹, and less on K¹⁰. One of the few K studies, a species-specific, small-scale investigation¹¹, attached importance to the development of biological K fertilizer and the screening of low-K tolerant genotypes. As field sampling is time-consuming and laborious, the basic statistical characteristics of K at larger scales are unknown, especially for communities. Importantly, the community, as the fundamental unit of the ecological model, offers insights into the structure and function of the ecosystem that are beyond the scope of the species level¹². Exploring the spatial pattern of plant K at the community can not only reflect changes in plant K, but also provide a reference for the optimization of ecosystem models.

Plant nutrient partitioning in organs is indicative of trade-off strategies deployed to acquire resources¹³. Factors such as climate and soil conditions influence the allocation and acquisition of K within plant organs¹⁴. In response to environmental changes, plants adjust the scaling relationship of elements among organs, a crucial adaptive mechanism. Based on these findings, scientists have proposed the *optimal partitioning hypothesis*, suggesting that plants prioritize nutrient allocation to organs with limited resource access in order to maximize growth rate¹⁵. For instance, in arid environments, plants optimize water and light utilization by accumulating higher K in leaves and roots, reducing transpiration in leaves, and enhancing water uptake by the roots^{3,16–18}. However, the *isometric partitioning hypothesis* takes the opposite view, proposing that nutrient allocation is determined solely by intrinsic plant characteristics, such as individual development, plant size, and physiological functioning, which are independent of environmental factors¹⁹. Consistent allometric growth relationships exist between different organs, maintaining relatively constant scaling exponents (*slopes*) despite variations in environmental conditions²⁰. Furthermore, studies have indicated a diminished influence of environmental factors when multiple species are involved^{21,22}. In light of these considerations, our study aims to explore the application of these allocation strategies to community-level K allocation in plants and to assess the extent to which environmental factors drive these patterns.

Accelerated by global warming, the plateau's warming rate has surpassed the global average²³. Consequently, the vegetation dynamics on the TP have experienced a surge in heterogeneity, leading to heightened uncertainty regarding the distribution of plant elements across different vegetation regions²⁴. Despite the importance of vegetation K in natural ecosystems, a comprehensive understanding of its spatial patterns remains lacking. Therefore, it is necessary to investigate the distribution characteristics of vegetation K in depth to fill this research gap and

contribute to the knowledge system of large-scale K-related research. Several theoretical hypotheses have been proposed to explain spatial patterns in element distribution. The *temperature-biogeochimistry hypothesis* posits that low temperatures reduce soil microbial activity, influencing soil nutrient availability, and subsequently reducing plant internal nutrient content²⁵. Conversely, the *temperature-plant physiology hypothesis* suggests that plants under low-temperature conditions require higher nutrient content to compensate for reduced physiological efficiency²⁵. While these hypotheses have been well-verified for N and P²⁶, their applicability to K research remains unexplored. Therefore, it is imperative to investigate the spatial variability of community K in different composition groups and across diverse environmental gradients to validate and enrich our scientific understanding of vegetation K characteristics under fluctuating environmental conditions and plant nutrient utilization strategies.

In this study, we consistently measured the K content and density of different plant organs in 2040 natural communities in the TP by gridding field samples as a 0.5° × 0.5° grid. We also explored the spatial patterns of K and its main driving factors at a large scale (Fig. 1). The main objectives of this study were: (1) to assess the K density within different community organs in the TP and analyze their allocation strategies, (2) to explore the drivers of vegetation K density and to predict the spatial distribution of different components, and (3) to calculate the K storage in the TP. This study provides validation for the *optimal partitioning hypothesis* and *isometric partitioning hypothesis* concerning plant K allocation. Additionally, it explores spatial distribution patterns and their correlation with environmental factors, encompassing the *temperature-biogeochimistry hypothesis* and *temperature-plant physiology hypothesis*. Emphasizing the significance of K factors in evaluating the impact of global change on nutrient cycling and large-scale mutual feedbacks is a crucial aspect of our findings. Furthermore, this study significantly enhances our comprehension of plant potassium nutrient utilization strategies along regional environmental gradients.

Methods

Study sites. The TP (73.43°–104.67°E, 25.98°–39.82°N), represents the world's highest plateau boasting an average elevation surpassing 4000 m, it is also known as the “third pole”. It exhibits a prominent elevation gradient, with elevated regions in the west and lower regions in the east²⁷. The plateau's topography is remarkably diverse, featuring a high plateau in the northern region, a canyon in the southern region, alpine valleys in the east, and the imposing Himalayan mountains in the west. Moreover, this region harbors diverse of ecosystems, including forests, shrublands, grasslands, and deserts²⁸.

The distinctive climate characteristics of the TP are shaped by the interactions of the Asian monsoon, westerly jet streams, and complex topographical features^{29,30}. The TP spans multiple climatic zones from tropical and subtropical to temperate, subfrigid, and frigid. In addition, this region exhibits a notable climate gradient^{31,32}; the annual radiation levels fluctuate between 11,277 and 17,581 kJ m⁻² day⁻¹, with an overall higher level of radiation; the annual mean temperature (MAT) ranges from -6 to 20 °C, displaying low interannual temperature differences but high diurnal temperature variations. Moreover, the annual mean precipitation (MAP) gradually increases from 20 millimeters in the northwest to 3042 millimeters in the southeast. Given its unique geographical location, diverse vegetation types, and rich climatic conditions, the TP serves as a distinctive “laboratory” for studying the dynamics of climate change in China.

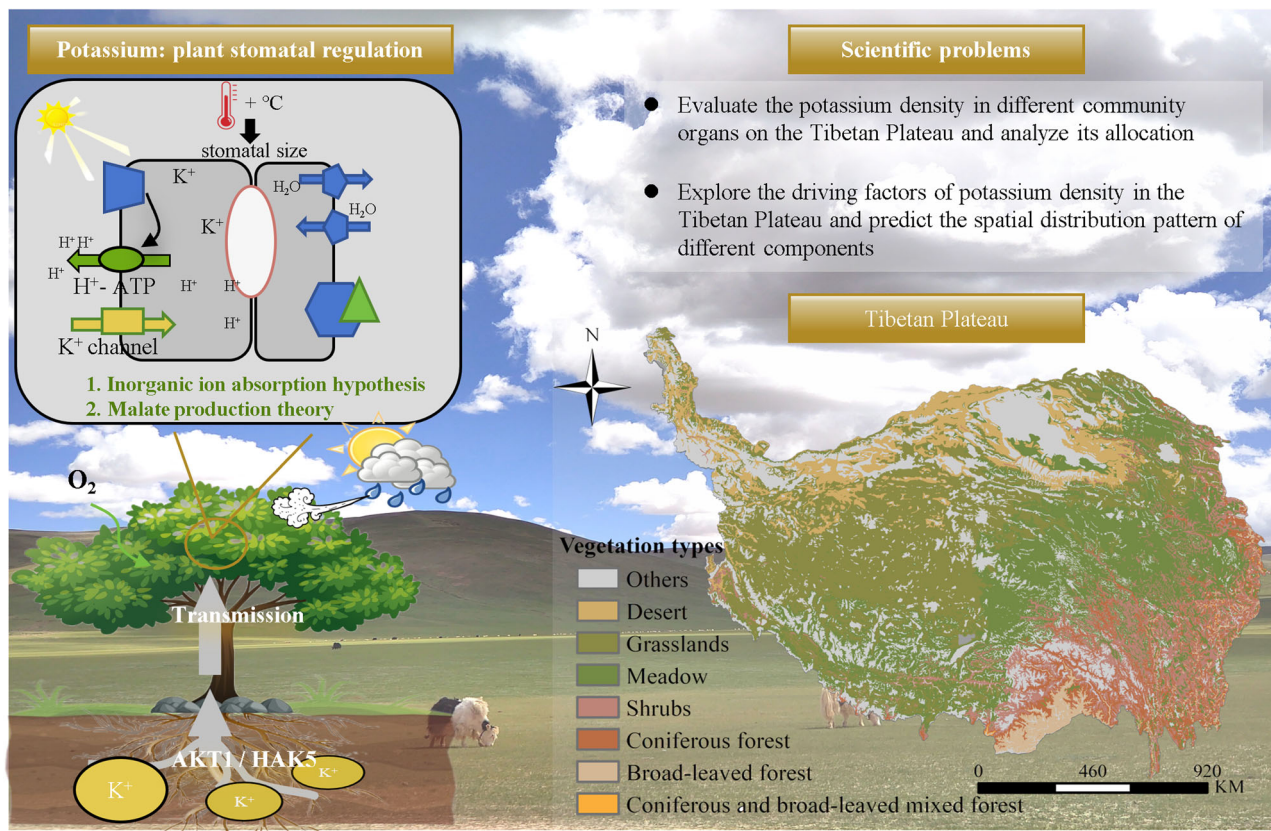


Fig. 1 Theoretical framework for spatial variation of vegetation potassium (K) density (g m^{-2}) in the Tibetan Plateau under climate change. The K density of plant communities was analyzed using consistently field-investigated data of 2040 plots (see Supplementary Fig. S1). The XY coordinate system of the map is the projection coordinate system of WGS_1984_Albers.

Field sampling. Field sampling was conducted from July to August 2019 to 2021. Systematic gridding field sampling was used to set up field sites at $0.5^\circ \times 0.5^\circ$ latitude and longitude. Based on the main types of vegetation in the TP, we set up field plots designated as four major groups, including forests, shrublands, grasslands, and deserts. A total of 2040 natural plant communities were investigated, among which 507 sites were from forests, 66 from shrubs, 69 from deserts, and 1398 from grasslands (Supplementary Fig. S1).

In order to assess the plant communities, at least three plots were set up at all sites (Supplementary Fig. S2), and the latitude, longitude, and altitude of each plot were recorded using GPS. The dominant plant communities were identified through visual observations made within each plot. In cases where more than one type of plant community was observed in a given plot, the vegetation type was randomly selected. In the forests (Supplementary Fig. S2), each site had three tree ($20 \text{ m} \times 20 \text{ m}$), three shrub ($5 \text{ m} \times 5 \text{ m}$) and three herb ($1 \text{ m} \times 1 \text{ m}$) quadrat. Firstly, the height (by tree altimeter) and diameter at breast height (by vernier caliper) of trees and shrubs were measured. Secondly, healthy, mature, and consistent species were considered, and organs were collected from each species (leaves, branches, trunk, and roots). In practice, the trunk was sampled using a growth cone with a diameter of 4.3 mm; the roots were dug out as completely as possible with a shovel and hoe. For the shrublands, a shrub and herb quadrat were assigned to each plot, and the same sampling methods were used as for tree quadrats. In the case of grassland and desert plots, the aboveground parts of all species in the squares ($1 \text{ m} \times 1 \text{ m}$) were sampled, and the roots were drilled with a 9 cm diameter soil auger to measure 0–30 cm of the root system. The aboveground part and the roots of the

grassland and desert samples were weighed, and this weight was recorded as the leaf and root biomass. Importantly, over 70% of the species present in all communities were collected. Furthermore, the 0–10 cm soil layer was sampled using a soil auger to measure the soil physical and chemical properties [soil organic carbon (SOC, %), N content (soil N, %), K content (soil K, %), and pH] in each plot.

Laboratory analyses. Plant samples were washed with deionized water, and the soil samples were cleaned to remove debris. All samples were then dried and ground using a chemical analysis ball mill (MM400 Ball Mill, Retsch, Germany) and an agate mortar grinder (RM200; Retsch, Germany). The K content of individual samples was determined using an inductively coupled plasma optical emission spectrometer (ICP-OES, Optima Avio 500, Perkin Elmer, Waltham, Massachusetts, United States), SOC and soil N were determined using an elemental analyzer (Vario Max CN elemental analyzer, Elemental, Germany), and soil pH was measured using a pH meter (Ultrameter II, USA).

Environmental variables. Based on the World Climate Database (Worldclim, <https://worldclim.org/data/index.html>), we extracted the mean annual temperature ($^\circ\text{C}$), growing season mean temperature ($^\circ\text{C}$), coldest month mean temperature ($^\circ\text{C}$), annual difference in temperature ($^\circ\text{C}$), MAP (mm), growing season precipitation (mm), wettest month precipitation (mm), driest month precipitation (mm), wind speed (m s^{-1}), and water vapor pressure (kPa). Solar radiation ($\text{mol m}^{-2} \text{d}^{-1}$), photosynthetic active radiation ($\text{mol m}^{-2} \text{d}^{-1}$), and ultraviolet radiation ($\text{MJ m}^{-2} \text{d}^{-1}$) were obtained based on the Science Data Bank (<https://doi.org/10.11922/sciencedb.332>).

The oxygen partial pressure (PO_2 , Pa) was calculated from altitude, according to the method of Kouwenberg et al.³³ as follows:

$$P = 101325 \left(\frac{MW_{air} \times g \times z}{R \times T} \right) \quad (1)$$

$$PO_2 = \left(\frac{P}{101325} \right) \times PO_{2,sea} \quad (2)$$

where, PO_2 (Pa) is calculated from altitude (z , in m) and mean July temperature (T , °C), MW_{air} is the molecular weight of air ($28.964 \times 10^{-3} \text{ kg mol}^{-1}$), g is the acceleration due to gravity in m s^{-2} , z is the altitude in m, R is the gas constant ($8.3144 \text{ J mol}^{-1}$), and T is calculated assuming a lapse rate of $0.6 \text{ °C per } 100 \text{ m}$ of altitude. $PO_{2,sea}$ is the PO_2 at sea level.

Calculation of biomass, K content, K density, and K storage.

The growth equation was used to determine the biomass of trees and shrubs using the measured DBH and tree height³⁴, calculated as follows (Supplementary Text S1):

$$B_{Com,i} = \sum_{i=1}^n \sum_{j=1}^m \frac{a_{i,j} D^{b_{i,j}}}{A} \quad (3)$$

where $B_{Com,i}$ is the community biomass density (kg m^{-2}) in organ i (leaf, branch, trunk, or root), $a_{i,j}$ and $b_{i,j}$ are constants for organ i of the specific tree or shrub species j . A is the area (m^2) of the sampling plot. n is the number of organs, and m is the number of plant species. The average biomass density of the three plots was calculated as the average biomass density at the sampling sites.

The K content (mg g^{-1}) of each organ was obtained via ICP-OES and then calculated by taking the mean value of the same organ for all species within the same plots; K density (g m^{-2}) is the product of K content (mg g^{-1}) and biomass (g m^{-2}). K storage (Tg) is the K density (g m^{-2}) multiplied by the occupied area (m^2) and is calculated as follows:

$$C_{Com,i} = \frac{\sum_{i=1}^n C_{Spe,i}}{n} \quad (4)$$

$$D_{Com,i} = \sum_{i=1}^n B_{Com,i} \times C_{Com,i} \quad (5)$$

$$S_{Com,i} = \sum_{i=1}^n D_{Com,i} \times A_j \quad (6)$$

where $C_{Com,i}$ is the K content (mg g^{-1}) within an organ (leaf, branch, stem, or root) of the community, and $C_{Spe,i}$ is the K content (mg g^{-1}) within an organ of the species in a tree or shrub. $D_{Com,i}$ is the K density per unit area (g m^{-2}), and $B_{Com,i}$ is the biomass per unit area (g m^{-2}). $S_{Com,i}$ is the K storage of a specific area (Tg), and A_j is the area (m^2), the calculation of which is based on the approach of Wu et al.³⁵

Statistical analysis. Differences in community K density among different organs and vegetation types were analyzed using one-way ANOVA with Excel 2010 and SPSS 21.0 (IBM, Chicago, IL, USA) software. Correlation analysis (R software)³⁶ and structural equation modeling (SEM) were used to analyze the relationship between K density and environmental factors. In the SEM analysis, the maximum likelihood estimate (MLE) was used to fit the data. The fit of the model was determined as follows: $P > 0.05$, ratio of cube to degrees of freedom (χ^2/df) = $1 - 3$, model fit (GIF) > 0.9 , and root mean square error (RMSEA) < 0.08 ³⁷. The biomass of trees and shrubs was calculated using the biomass equation. An allometric model was used to explore K^+ density

distribution in different organs. The K densities of the different components were predicted using the random forest model³⁸. Statistical significance was set at $P < 0.05$.

The allometric model is a statistical mathematical method used to explore vegetation growth strategies. In the allometric relationship, the distribution relationship in different plant organs can be expressed using the equation:

$$Y = bX^a \quad (7)$$

where a is the allometric scaling component (*slope*), and b is the allometric growth coefficient (*intercept*). When $a = 1$ and its value is significant, or when $a \neq 1$ and its value is not significant, it is considered to imply isomeric allocation. Other cases imply allometric allocation. When $a > 1.0$, the increase in Y is greater than the increase in X , and vice versa when $a < 1.0$. X and Y represent the K density in specific organs (D_{leaf} , D_{branch} , D_{trunk} , and D_{root}). The parameters were fitted using the “lmodel2” function in the “lmodel2” package in R³⁹. The likelihood ratio test was used to determine significant differences in the allometric growth index (a) between different plant growth types of the same organ in pairs. The test was performed using the “sma” function of the “smatr” package in R⁴⁰.

The spatial distribution of K content and vegetation density in the TP were estimated using the random forest (RF) algorithm³⁸ and MATLAB 2018b software (version 2018b; MathWorks, Natick, MA, USA). The spatial distribution map of the field investigation was produced using ArcGIS (Version 10.2, ESRI Press, Redlands, CA, USA). Random forest is a combinatorial classifier algorithm proposed by Breiman (2001), composed of many single classification and regression trees. The bootstrap resampling method was used to extract multiple samples from the original samples, and decision-tree modeling was performed for each bootstrap sample. Finally, the classification results were determined using the voting method. The generation of a single tree depends on an independent, identically distributed random vector. The overall generalization error depends on the classification efficiency of a single tree in the forest and the correlation between classification trees.

Results

Changes in K content and density among different organs and their allocation. The data from 2040 sites in the TP showed average K contents for leaves, branches, trunks, and roots of 16.05 (C_{leaf}), 3.91 (C_{branch}), 1.46 (C_{trunk}), and 4.03 mg g^{-1} (C_{root}), respectively. The K content was significantly different among different plant organs ($P < 0.01$), the highest of which was observed in C_{leaf} (Fig. 2).

Furthermore, the K density was significantly different among the different organs ($P < 0.05$). The K density of leaves (D_{leaf}), branches (D_{branch}), trunks (D_{trunk}), and roots (D_{root}) were estimated to be 6.07, 12.84, 10.39, and 4.86 g m^{-2} , respectively, with branches (D_{branch}) showing the highest density (Fig. 3).

Scaling relationships of K among leaves, branches, trunks, and roots. The allometric growth equation results (Table 1) showed an allometric relationship among all organs in total, except for a special isomeric relationship distribution in the desert. The scaling exponent (*slope*) of D_{leaf} vs. D_{root} in the forest, shrubland, and grassland was 0.71, 0.70, 0.67, all less than one, and greater than 1 in desert, but not significant ($P = 0.54$). The changing of K was fastest in leaves and relatively slower in roots in the forest, shrubland, and grassland, but this condition was reversed in the desert.

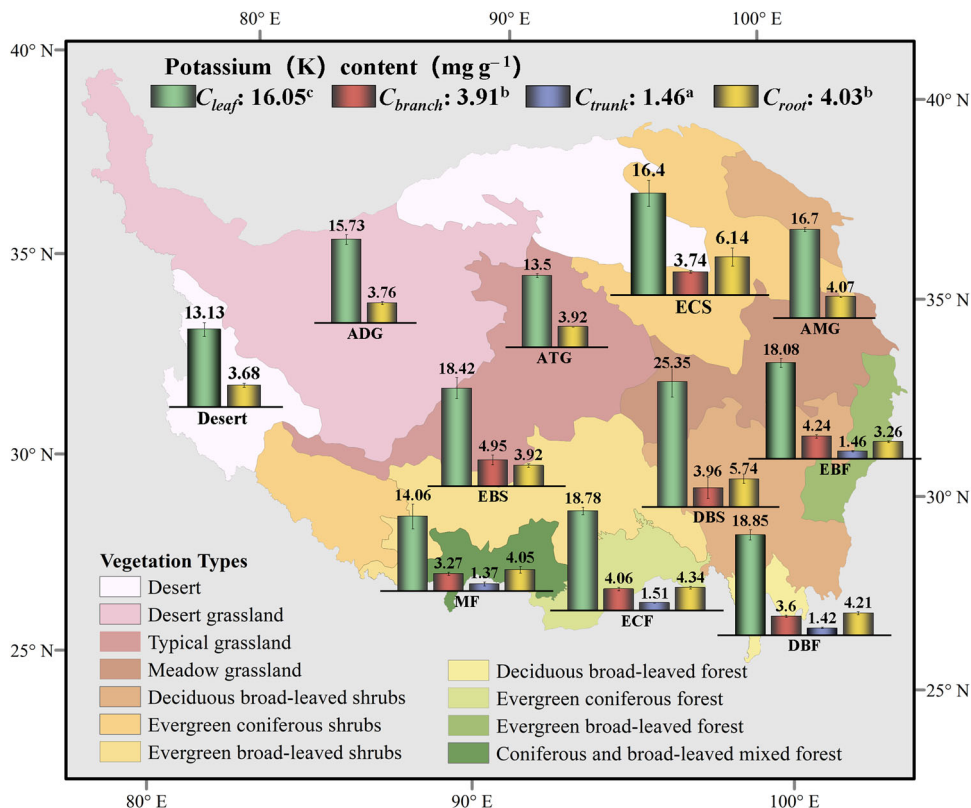


Fig. 2 Changes in potassium (K) content (mg g⁻¹) among plant organs across different vegetation types. The four values at the top of the figure represent the average K content of different organs, different lowercase letters indicate significant differences between the organs in each column at $P < 0.05$. Different color columns in the map represent K content in different organs of different vegetation types (green: leaves, pink: branches, blue-violet: trunk, and brown: roots). Vegetation zoning is based on the dominant vegetation type with reference to vegetation types found in China. The XY coordinate system of the map is the projection coordinate system of WGS_1984_Albers. C_{leaf} : leaf K density (mg g⁻¹); C_{branch} : branch K density (mg g⁻¹); C_{trunk} : trunk K density (mg g⁻¹); C_{root} : root K density (mg g⁻¹). EBF evergreen broad-leaved forest, ECF evergreen coniferous forest, DBF deciduous broad-leaved forest, MF coniferous and broad-leaved mixed forest, EBS evergreen broad-leaved shrubs, ECS evergreen coniferous shrubs, DBS deciduous broad-leaved shrubs, AMG alpine meadow grassland, ATG alpine typical grassland, ADG alpine desert grassland.

Response of vegetation K density to environmental variation.

According to the SEM results (Supplementary Fig. S4), the total vegetation K density at the community level was mainly influenced by precipitation. Of these, path analysis showed that environmental factors explain 29% of the variation in D_{leaf} , and D_{leaf} was mainly influenced by radiation, precipitation, and PO_2 , with precipitation being the main environmental driver (Fig. 4). In different community types (Fig. 5 and Supplementary Fig. S5), the main environmental factors influencing the spatial variation of D_{leaf} were different as well. Linear regression correlation analysis (Supplementary Figs. S6 and S7) showed that precipitation and temperature were significantly and positively correlated with D_{leaf} . These results were also verified via analyses of the different climate zones (Supplementary Fig. S7), showing higher K density in plants in warm and humid regions.

Spatial distribution of vegetation K in TP. The spatial distribution of K density can be well depicted for different components in the random forest model, especially for aboveground and total vegetation K density (Supplementary Fig. S11, $R^2 = 0.78$). In addition, K density showed a decreasing trend from southeast to northwest (Fig. 6), as the vegetation types in the TP gradually changed from forest to shrubland, grassland, and desert, with K densities of 44.01 g m⁻², 35.32 g m⁻², 4.08 g m⁻², and 3.41 g m⁻², respectively (Table 2). Overall, natural vegetation in the TP stores 19.92 Tg of K, where 13.15 Tg K is stored in the aboveground vegetation, and 6.77 Tg K is stored belowground.

Discussion

Variation in plant K on the TP. Utilizing data obtained from a comprehensive analysis of 2040 plant sites, our study represents a pioneering effort in estimating the K content and density within the TP vegetation. In terms of K content, prior investigations conducted by Han et al.⁴¹ demonstrated an average leaf K content (C_{leaf}) of 11.48 mg g⁻¹ in China, while Li et al.¹⁰ reported a C_{leaf} of 20.22 mg g⁻¹ in the TP. According to our grid sampling results in the TP, C_{leaf} was 16.05 mg g⁻¹ (Fig. 2), which was higher than that of Han et al.⁴¹. This discrepancy could potentially be attributed to the distinctive climatic characteristics of the Tibetan region, the physiological functionality of K, and the different data acquisition methods. Our research focused on the alpine region, which encompasses a diverse range of extreme environments characterized by lower temperatures, increased radiation levels, and shorter growing seasons⁴². Higher C_{leaf} helps to extend plant leaf longevity and improves its resilience to stressful environments³: as levels of reactive oxygen species (ROS) increase dramatically due to environmental stresses (e.g., UV light or low temperatures and cause severe damage to cellular structures, K can effectively mitigate ROS production¹⁶. Apart from this, we posit that the reason behind the lower outcomes observed in comparison to Li et al.¹⁰ may be attributed to the augmented coefficient of variation among the various sampled species, such as the differences in K nutrient requirements during plant growth and development under different environmental conditions such as water, light, and nutrients,

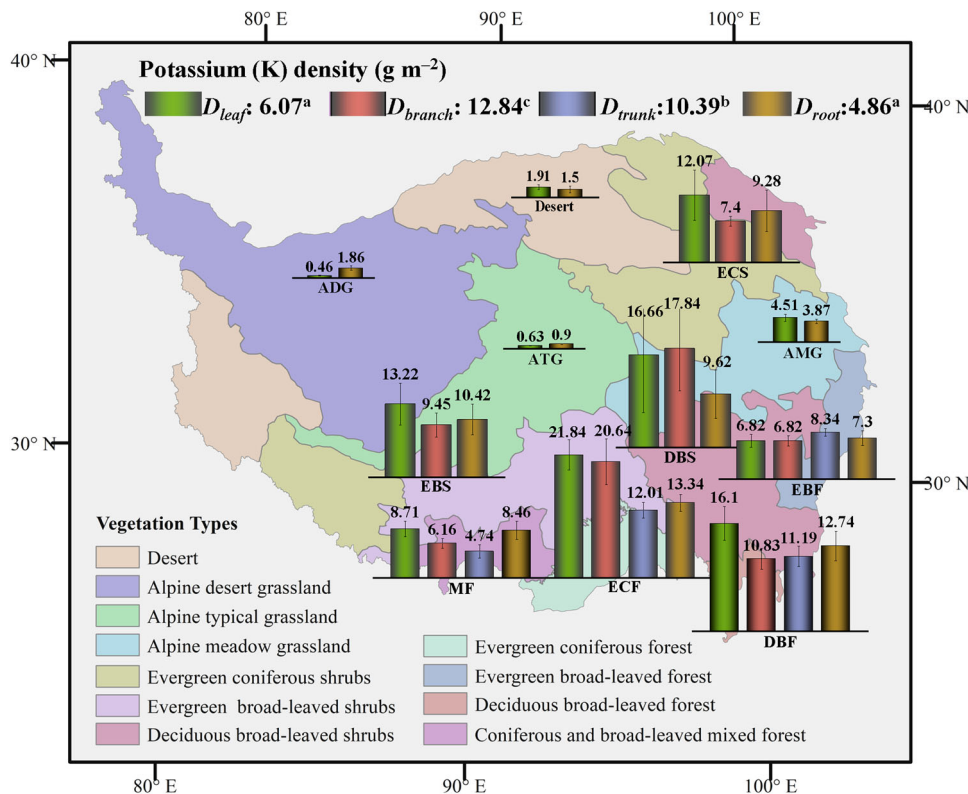


Fig. 3 Variations in potassium (K) density (g m^{-2}) among plant organs across different vegetation types on the Tibetan Plateau. The four values at the top of the picture represent the average K density of different organs, different lowercase letters indicate significant differences among the organs in each column at $P < 0.05$. Different color columns in the map represent K densities in different organs of different vegetation types (green: leaves, pink: branches, blue-violet: trunk, and brown: roots). Vegetation zoning is based on the dominant vegetation type with reference to vegetation types found in China. The XY coordinate system of the map is the projection coordinate system of WGS_1984_Albers. D_{leaf} : leaf K density (g m^{-2}); D_{branch} : branch K density (g m^{-2}); D_{trunk} : trunk K density (g m^{-2}); D_{root} : root K density (g m^{-2}). EBF evergreen broad-leaved forest, ECF evergreen coniferous forest, DBF deciduous broad-leaved forest, MF coniferous and broad-leaved mixed forest, EBS evergreen broad-leaved shrubs, ECS evergreen coniferous shrubs, DBS deciduous broad-leaved shrubs, AMG alpine meadow grassland, ATG alpine typical grassland, ADG alpine desert grassland.

Table 1 Key parameters of allometric equations for potassium (K) density (g m^{-2}) in plant communities of the Tibetan Plateau.

Communities	Organs (x vs. y)	No.	R ²	P	Slope	95% CI	Intercept	95% CI	
Forest	D_{leaf} vs. D_{branch} [¶]	169	0.46	0 < 0.001	1.19	(1.06, 1.33)	-5.42	(-8.8, -2.04)	***,‡
	D_{leaf} vs. D_{trunk}	169	0.53	0 < 0.001	0.54	(0.49, 0.60)	1.92	(0.5, 3.35)	***
	D_{leaf} vs. D_{root}	169	0.48	0 < 0.001	0.71	(0.64, 0.80)	0.29	(-1.69, 2.26)	***
	D_{branch} vs. D_{trunk}	169	0.39	0 < 0.001	0.45	(0.40, 0.51)	4.38	(2.91, 5.86)	***
	D_{branch} vs. D_{root}	169	0.25	0 < 0.001	0.60	(0.53, 0.68)	3.54	(1.31, 5.77)	***
	D_{trunk} vs. D_{root}	169	0.34	0 < 0.001	1.32	(1.17, 1.50)	-2.26	(-4.74, 0.23)	***
Shrubland	D_{leaf} vs. D_{branch}	22	0.14	0.08	0.56	(0.37, 0.85)	2.52	(-2.53, 7.58)	**
	D_{leaf} vs. D_{root}	22	0.85	0 < 0.001	0.70	(0.59, 0.85)	0.36	(-2.11, 2.83)	***
	D_{branch} vs. D_{root}	22	0.05	0.33	1.26	(0.81, 1.96)	-2.82	(-10.75, 5.12)	ns
Grassland	D_{leaf} vs. D_{root}	466	0.63	0 < 0.001	0.67	(0.63, 0.71)	0.77	(0.48, 1.05)	***
Desert	D_{leaf} vs. D_{root}	23	0.02	0.54	1.51	(0.97, 2.33)	-1.38	(-3.56, 0.8)	ns
Total	D_{leaf} vs. D_{branch}	191	0.44	0 < 0.001	1.16	(1.04, 1.29)	-4.97	(-8.07, -1.88)	**
	D_{leaf} vs. D_{trunk}	169	0.53	0 < 0.001	0.54	(0.49, 0.60)	1.92	(0.5, 3.35)	***
	D_{leaf} vs. D_{root}	680	0.62	0 < 0.001	0.70	(0.67, 0.73)	0.62	(0.15, 1.09)	***
	D_{branch} vs. D_{trunk}	169	0.39	0 < 0.001	0.45	(0.40, 0.51)	4.38	(2.91, 5.86)	***
	D_{branch} vs. D_{root}	191	0.24	0 < 0.001	0.62	(0.54, 0.70)	3.35	(1.28, 5.43)	***
	D_{trunk} vs. D_{root}	169	0.34	0 < 0.001	1.32	(1.17, 1.50)	-2.26	(-4.74, 0.23)	***

R² coefficient of determination, CI confidence interval.
 ‡ ***, ** denote significant differences between the slope of the equation and 1 at $P = 0.001$ and 0.01 ; ns, no significant difference at $P = 0.05$.
 ¶ D_{leaf} : leaf potassium density (g m^{-2}); D_{branch} : branch potassium density (g m^{-2}); D_{trunk} : trunk potassium density (g m^{-2}); D_{root} : root potassium density (g m^{-2}).
 The K density of different plant organs was transformed into a log-log scale. The likelihood test was used to examine differences among different organs, and the data were analyzed using a standardized major axis and calculated using SMATR Version 2.0 (<http://www.bio.mq.edu.au/ecology/SMATR/>).

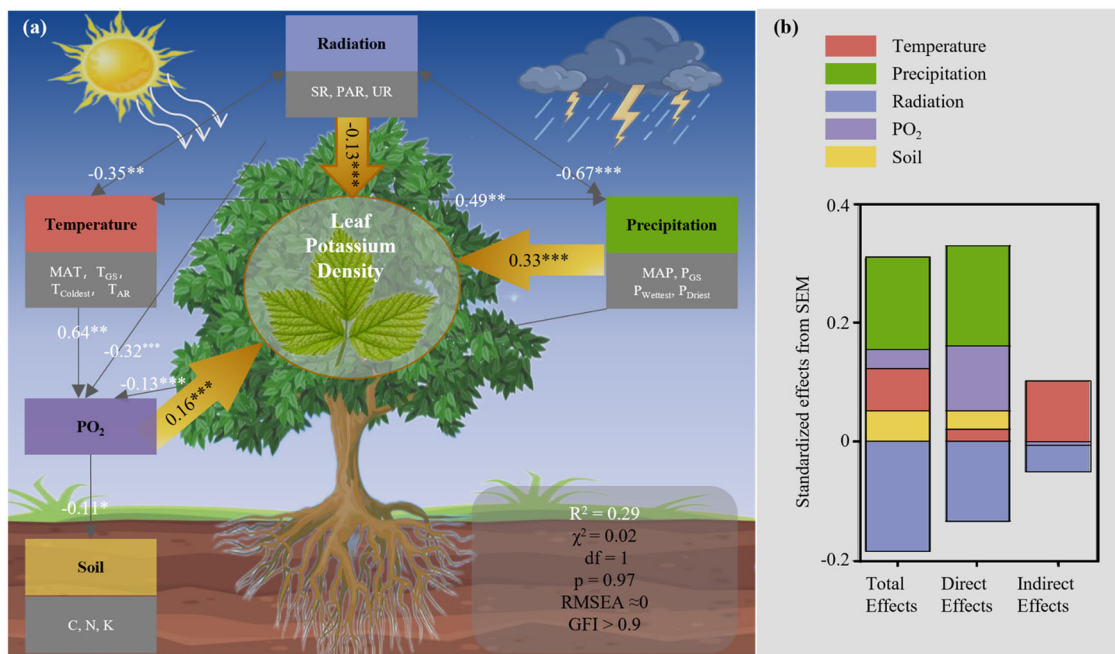


Fig. 4 Path analysis exploring direct and indirect effects of environmental factors on the spatial distribution of potassium (K) density in leaves. (a) Linear relationship between leaf potassium density and environmental factors. (b) the effects of environmental factors on leaf K density.

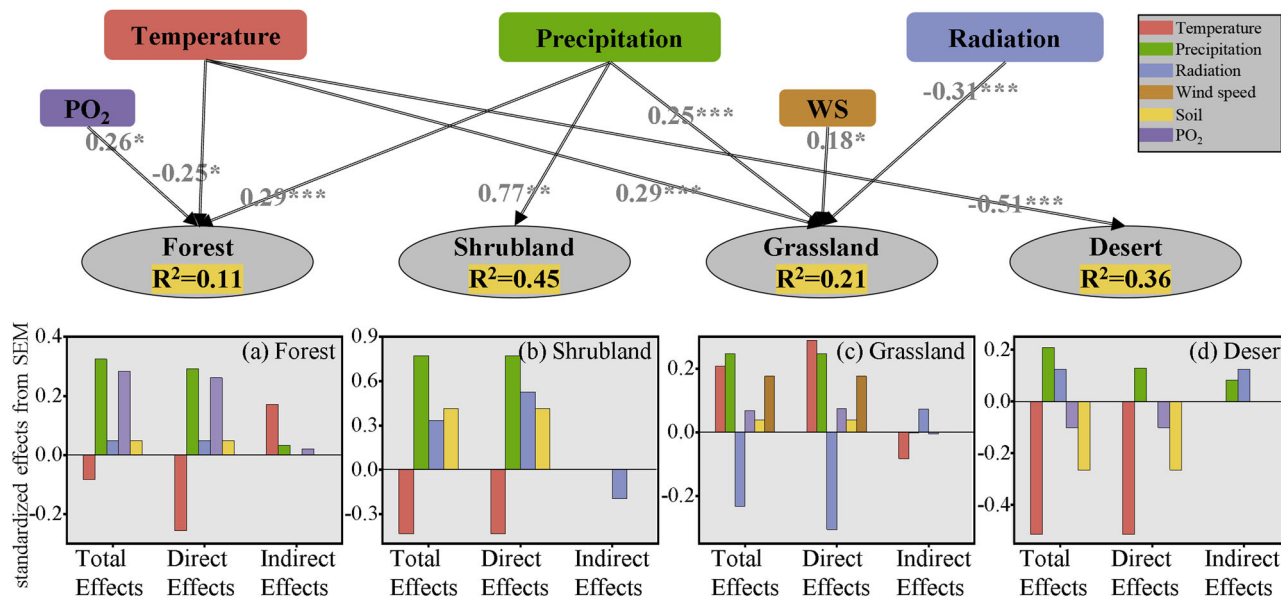


Fig. 5 Path analysis exploring the effects of environmental factors on the spatial distribution of potassium (K) density in leaves of different communities and the direct and indirect effects of environmental factors on leaf K density. (a) is in the forest, (b) is in the shrubland, (c) is in the grassland and (d) is in the desert.

resulting in differences in leaf K among different plant species in different habitats^{43,44}. Moreover, different sampling methods, measurements, and species composition could also yield disparate outcomes⁴⁰.

The average K density of vegetation in the TP was approximately 21.71 g m⁻² (Table 2). Furthermore, our analysis revealed significant variations ($P < 0.01$) in K density across different plant organs, with the density in branches (D_{branch}) being the highest (Fig. 3). Interestingly, only in evergreen broad-leaved forests (Table 2 and Fig. 2), where more K is allocated proportionally to wood than to leaves ($D_{branch} > D_{leaf}$),

lower K density in leaves is usually associated with lower growth, reflecting the slow growth and conservative lifestyle of plants¹⁴.

Optimal partitioning strategy shapes K density allocation among diverse plant communities. When faced with limited environmental resources, the allocation of these resources among different plant organs often leads to conflicts, giving rise to selective allocation, which adheres to the principle of *optimal partitioning*^{19,45}. The allocation of K is defined in our study as a change in allometric curves, and at a different scaling exponent (*slope*). Among these, the *slope* of D_{leaf} vs. D_{root} was < 1.0 in the

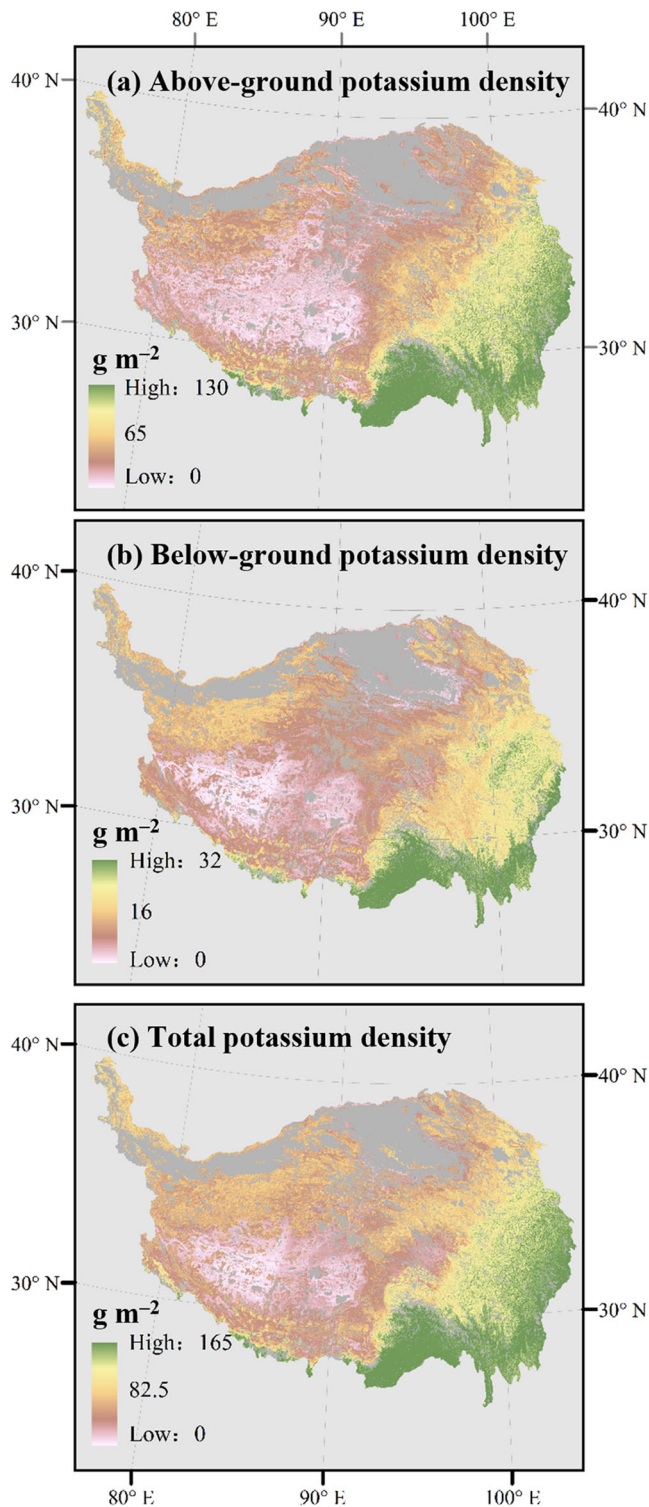


Fig. 6 Predicted spatial patterns of vegetation potassium (K) density (g m^{-2}) on the Tibetan Plateau with a resolution of 1 km. Spatial distribution of K density in **a** aboveground, **b** belowground, and **c** total vegetation. The XY coordinate system of the map is the projection coordinate system of WGS_1984_Albers.

forest, shrubland, and grassland (Table 1), probably due to the fact that plants tend to pay more attention to the allocation of leaf resources, in order to maximize light-acquisition capacity, and increase productive capacity⁴⁶. Furthermore, the slopes of D_{leaf} vs. D_{root} in the above three communities were 0.71 (forest), 0.70

Table 2 Changes in potassium (K) density (g m^{-2}) and storage between different vegetation types in the Tibetan Plateau.

Communities	Vegetation types	Area (10^4 km^2)	K content (mg g^{-1})			K density (g m^{-2})			K storage (T g)			
			Leaf	Branch	Trunk	Leaf	Branch	Trunk	Leaf	Branch	Trunk	Total
Forest	EBF	1.35	18.08	4.24	1.46	6.82	6.82	0.09	0.09	0.11	0.10	0.40
	ECF	15.57	18.78	4.06	1.51	21.84	20.64	3.40	3.21	1.87	2.08	10.56
	DBF	0.18	18.85	3.60	1.42	16.10	10.83	0.03	0.02	0.02	0.02	0.09
	MF	0.42	14.06	3.27	1.37	8.71	6.16	0.04	0.03	0.02	0.04	0.12
Shrubland	Total	17.51	17.44	3.79	1.44	13.37	11.11	2.34	1.95	1.59	1.83	7.71
	EBS	2.32	18.42	4.95	1.44	13.22	9.45	0.31	0.22	0.24	0.24	0.77
	ECS	0.72	16.40	3.74	1.44	12.07	7.40	0.09	0.05	0.07	0.07	0.21
	DBS	14.78	25.35	3.96	1.44	16.66	17.84	2.46	2.64	1.42	1.42	6.52
Grassland	Total	17.82	20.06	4.21	1.44	13.98	11.56	2.49	2.06	1.74	1.06	6.29
	AMG	27.47	16.70	4.07	1.44	4.51	3.87	1.24	1.24	1.06	1.06	2.30
	ATG	53.4	13.50	3.92	1.44	0.63	0.90	0.34	0.34	0.48	0.48	0.82
	ADG	63.07	63.07	3.76	1.44	0.46	1.86	0.29	0.29	1.47	1.47	3.18
Desert	Total	143.94	15.31	3.92	1.44	1.87	2.21	2.69	4.08	3.18	3.18	5.87
	Desert	1.41	13.13	3.68	1.44	1.91	1.50	0.03	0.03	0.02	0.02	0.05
Total	Total	180.68	16.49	4.00	1.44	7.78	11.34	7.55	4.01	1.59	6.77	19.92

EBF evergreen broad-leaved forest, ECF evergreen coniferous forest, DBF deciduous broad-leaved forest, MF coniferous and broad-leaved mixed forest, EBS evergreen coniferous shrubs, ECS evergreen coniferous shrubs, DBS deciduous broad-leaved shrubs, AMG alpine meadow grassland, ATG alpine typical grassland, ADG alpine desert grassland.
 *Data support from Geographic Data Sharing Infrastructure, College of Urban and Environmental Science (<http://geodata.pku.edu.cn>).

(shrubland), and 0.67 (grassland), not much of a difference, suggesting that the allocation of plant leaves and roots in these communities was stable, and that nutrient allocation strategy of the plant was more conservative³⁹.

On the contrary, the desert exhibited distinctive isomeric K allocation patterns (Table 1), with a scaling exponent (*slope*) for D_{leaf} vs. D_{root} of 1.51. This unique allocation strategy in the desert can be attributed to its extreme environmental conditions such as drought, freezing temperatures, and large diurnal temperature variations. In response to these challenges, plants in the desert enhance their roots to improve nutrient uptake, allocating more K to roots to enhance passive water uptake capacity, increase cell turgor pressure, and enhance resistance to desiccation, thereby improving drought tolerance¹⁶. In addition, K^+ ions play a crucial role in stimulating the activity of carbohydrate-metabolizing enzymes in roots⁴⁷. Together, they regulate the permeability of cells and increase the stability of cell membranes to prevent intracellular freezing at low temperatures and reduce water loss at high temperatures^{17,48}. In summary, the distinctive isomeric allocation patterns of D_{leaf} and D_{root} observed in the desert, along its *slope*, which is inconsistent compared to that of the forest, shrubland, and grassland. These findings suggest that the observed K allocation patterns may be a response to specific environments, such as drought and low temperatures, to achieve the optimal optimization of resources.

Driving factors on the spatial variation of vegetation K density in the TP. Poorter and Nagel⁴⁹ demonstrated the plasticity of spatial variation in plant nutrition and the potential impact of environmental changes on this variation. Through the utilization of SEM and linear regression (Fig. 4 and Supplementary Fig. S4), precipitation emerged as a significant environmental driver for spatial variation in vegetation K density on the TP, showing a positive correlation with K density. Notably, plants in humid regions exhibited higher K density (Supplementary Figs. S6 and S7), which can enhance their ability to resist waterlogging by increasing the passive transport of K^3 . The *temperature-biogeochemistry hypothesis* hold that soil nutrient availability primarily determines plant nutrition distribution. Traditionally, soil nutrients have been recognized as the primary regulators of plant K^{50,51}. In contrast, our study reveals that the impact of soil K is relatively minor (Fig. 4 and Supplementary Figs. S4, S6, and S7). The *temperature-biogeochemistry hypothesis* was not well tested in our study. In addition, according to this hypothesis *temperature-plant physiology hypothesis*, it is logical that the lower the temperature, the higher the plant K content. However, in contradiction to this, our results (Supplementary Figs. S4–S7) show that, the higher the temperature, the higher the K in the leaves. This inconsistency can be rationalized by the fact that suitable temperatures promote essential physiological processes like photosynthesis and transpiration. These processes require more K to activate relevant enzymes and facilitate the synthesis and transportation of amino acids, proteins, and carbohydrates⁵².

However, when considering the relatively low coefficient of determination ($R^2 < 45\%$), in conjunction with the consistent support for the *stability of limiting hypothesis*⁴¹ and the *stoichiometric homeostasis theory*⁵³, the factors that remain unexplained could potentially be attributed to the maintenance of homeostasis in plants. Additionally, these unexplained factors might be associated with other overlooked variables, such as the impact of iceberg snowmelt on soil water content, which would subsequently influence the capacity of plant roots to uptake K^{54,55}. Furthermore, it is worth noting that the effects of plant taxonomy, phylogeny, and the intraspecific variation of functional traits caused by the water-energy dynamic changes brought

about by the altitude of the TP are also crucial factors influencing the investigation of environmental drivers in relation to plant K dynamics (ref.^{56,57}; Sigdel et al. 2023). Consequently, there is an imperative to cultivate a more comprehensive understanding of the mechanisms underlying environmental drivers of plant K, as it contributes to the advancement of our knowledge regarding material cycling and energy flux in terrestrial ecosystems.

The combination of grid sampling with the model accurately predicts the spatial map of vegetation K on the TP. The combination of grid sampling with the RF model greatly improved K density estimation. Previous studies estimating elemental content and density only used a linear regression model^{10,41}. Thus, the covariance problem of multiple linear regression models and the accuracy of model fitting were significantly affected⁵⁸. Moreover, numerous theoretical and empirical studies have demonstrated that RF has a high prediction accuracy. RF has good tolerance to outliers and noise, and it is not prone to overfitting⁵⁹. Here, we used uniform and standardized grid sampling, which evenly distributes the sampling points. The community K density data were measured by us, rather than integrated, which should also reduce the error of the transmission process to some extent.

Based on the results of the constructed RF (Fig. 6 and Supplementary Figs. S9 and S10), the predicted values matched well with the true values, and the accuracy of the fitting process was high. This implies a strong correlation between K density and the screened environmental factors, and the selected independent variables could initially reflect the information of the community K density in general. The spatial distribution of K content and density of each component in the TP with a resolution of 1 km (Fig. 6 and Supplementary Fig. S8) showed a decreasing trend from the southeast to northwest, which is consistent with the results obtained using direct statistical methods (Table 2). However, some uncertainties remain in the estimation process: The environmental data quality, errors introduced in the raw data, and data processing should result from some uncertainty. Moreover, according to direct statistical methods, the total K storage in vegetation on the TP was estimated in this study to be 19.92 Tg in this study, of which 7.71, 6.29, 5.87, and 0.05 Tg were stored in the forest, shrubland, grassland, and desert, respectively (Table 2). In addition, forests are the largest K reservoir on the TP, which may be closely related to their high K density. However, since the area is extracted from Wu et al.³⁵ and is not an actual measurement, the accuracy has to be considered. Importantly, this is the first assessment of K storage on the TP to date, and the datasets of K content and density at the regional level should be used as input parameters or initial variables for global K-cycle models and as calibration data.

Conclusions

The K content, density, and storage of vegetation in the TP were evaluated using systematic investigation data from 2040 natural plant communities. At the community level, K contents in the leaf, branch, trunk, and root were estimated at 16.05, 3.91, 1.46, and 4.03 mg g⁻¹, respectively, and the K density in these organs was 6.07 (D_{leaf}), 12.84 (D_{branch}), 10.39 (D_{trunk}), and 4.86 (D_{root}) g m⁻². Furthermore, within the context of scaling relationships, the allocation strategy of K density among different plant organs and communities has been widely observed. Plants in desert adopt specific isomeric strategies to adapt to various low-temperature and arid environments. For environmental drivers, precipitation, radiation, and PO₂ are identified as the primary environmental factors driving variations in K density. The positive correlation of K density with precipitation and temperature arises from the role of K^+ in regulating osmotic pressure,

stimulating enzyme activity, enhancing photosynthesis, and promoting protein amino acid synthesis, among other physiological functions. Regarding spatial distribution, both K content and density exhibited a trend of higher values in the southeast and lower values in the northwest. Leveraging the random forest model, we effectively captured the spatial patterns of K density on the TP at a 1 km resolution, achieving an accuracy exceeding 70%. Our research findings further underscore the fundamental significance of K, especially in the context of the TP, as well as the response of plant K to future global changes. These insights should contribute significantly to substantial improvements in existing earth system models that are related to these factors.

Data availability

The data of K are available from the National Tibetan Plateau Data Center at <https://doi.org/10.11888/Terre.tpd.272420> and <https://doi.org/10.11888/Terre.tpd.272695>.

Received: 7 December 2022; Accepted: 29 September 2023;

Published online: 11 October 2023

References

- Wright, S. J. et al. Potassium, phosphorus, or nitrogen limit root allocation, tree growth, or litter production in a lowland tropical forest. *Ecology* **92**, 1616–1625 (2011).
- Lucanus, B. Versuche über die umwandlung salpetersaurer Alkalien in Chloride. *Fresenius Zeitschrift F. Anal. Chemie* **3**, 403–405 (1864).
- Sardans, J. & Peñuelas, J. Potassium: a neglected nutrient in global change. *Glob. Ecol. Biogeogr.* **24**, 261–275 (2015).
- Thornburg, T. E. et al. Potassium deficiency significantly affected plant growth and development as well as microRNA-mediated mechanism in wheat (*Triticum aestivum* L.). *Front. Plant Sci.* **11**, 1219 (2020).
- Xia, L. Physiological effect of potassium and cause analysis of soil potassium deficiency (in Chinese). *Mod. Agric.* **02**, 42–43 (2016).
- Tan, D. S., Jin, J. Y., Jiang, L. H., Huang, S. W. & Liu, Z. H. Potassium assessment of grain producing soils in North China. *Agric. Ecosyst. Environ.* **148**, 65–71 (2012).
- Zhang, Y. L., Li, B. Y. & Zheng, D. A. A discussion on the boundary and area of the Tibetan Plateau in China. *Geographical Research* (in Chinese), **21**, 1–8 (2002).
- Deng, T., Wu, F. X., Zhou, Z. K. & Su, T. Tibetan Plateau: an evolutionary junction for the history of modern biodiversity. *Sci. China Earth Sci.* **63**, 172–187 (2019).
- Zhang, J. H. et al. Leaf N:P ratio does not predict productivity trends across natural terrestrial ecosystems. *Ecology* **103**, e3789 (2022).
- Li, X., He, N. P., Xu, L., Li, S. G. & Li, M. X. Spatial variation in leaf potassium concentrations and its role in plant adaptation strategies. *Ecol. Indic.* **130**, 108063 (2021).
- Ye, Z. L., Zeng, J. B., Ma, X. Y., Long, L. Z. & Zhang, G. P. Transcriptome profiling analysis reveals involvement of SAM cycle and methionine pathway in low potassium tolerance in barley. *Curr. Plant Biol.* **25**, 100190 (2021).
- He, N. P. et al. Ecosystem traits linking functional traits to macroecology. *Trends Ecol. Evol.* **34**, 200–210 (2019).
- Reich, P. B. et al. Evidence of a general 2/3-power law of scaling leaf nitrogen to phosphorus among major plant groups and biomes. *Proc. Royal Soc. B Biol. Sci.* **277**, 877–883 (2010).
- Sardans, J. et al. Stoichiometry of potassium is largely determined by water availability and growth in Catalonian forests. *Funct. Ecol.* **26**, 1077–1089 (2012).
- Peng, Y. et al. Globally limited individual and combined effects of multiple global change factors on allometric biomass partitioning. *Global Ecol. Biogeogr.* **31**, 454–469 (2021).
- Abbasi, G. H. et al. Potassium application mitigates salt stress differentially at different growth stages in tolerant and sensitive maize hybrids. *Plant Growth Regul.* **76**, 111–125 (2015).
- Hu, W. et al. Potassium application affects carbohydrate metabolism in the leaf subtending the cotton (*Gossypium hirsutum* L.) boll and its relationship with boll biomass. *Field Crops Res.* **179**, 120–131 (2015).
- Kafkafi, S. K. K. Potassium and abiotic stresses in plants. In: Surya Kant & Uzi Kafkafi (eds) *Potassium for Sustainable Crop Production*. 233–251 (Potash Institute of India, 2002).
- Liu, R. et al. Allometry rather than abiotic drivers explains biomass allocation among leaves, stems and roots of *Artemisia* across a large environmental gradient in China. *J. Ecol.* **109**, 1026–1040 (2020).
- Niklas, K. J. Plant allometry: is there a grand unifying theory? *Biol. Rev. Cambridge Philos. Soc.* **79**, 871–889 (2004).
- He, J. S. et al. Stoichiometry and large-scale patterns of leaf carbon and nitrogen in the grassland biomes of China. *Oecologia* **149**, 115–122 (2006).
- Zhao, W. Q. et al. Shrub type dominates the vertical distribution of leaf C:N:P stoichiometry across an extensive altitudinal gradient. *Biogeosciences* **15**, 2033–2053 (2018).
- Mao, G. N. et al. Monsoon affects the distribution of antibiotic resistome in Tibetan glaciers. *Environ. Pollut.* **317**, 120809 (2023).
- Cai, Q. et al. Distribution patterns and driving factors of leaf C, N and P stoichiometry of coniferous species on the eastern Qinghai-Xizang Plateau, China. *Chinese J. Plant Ecol.* **42**, 1048–1060 (2019).
- Reich, P. B. & Oleksyn, J. Global patterns of plant leaf N and P in relation to temperature and latitude. *Proc. Natl. Acad. Sci. USA* **101**, 11001–11006 (2004).
- Yang, X. Variations of plant N, P concentrations in shrubland biomes across northern China: phylogeny, climate and soil. *Biogeosciences* **13**, 4429–4438 (2016).
- Shen, X. J. et al. Asymmetric impacts of diurnal warming on vegetation carbon sequestration of marshes in the Qinghai Tibet Plateau. *Glob. Biogeochem. Cycles* **36**, e2022GB007396 (2022).
- Chen, F. H. et al. The Tibetan Plateau as the engine for Asian environmental change: the Tibetan Plateau Earth system research into a new era. *Sci. Bull.* **66**, 1263–1266 (2021).
- Huang, L. X. et al. The northern boundary of the Asian summer monsoon and division of westerlies and monsoon regimes over the Tibetan Plateau in present-day. *Sci. China Earth Sci.* **53**, 866–878 (2023).
- Ren, Y. H. et al. The south Asia monsoon break promotes grass growth on the Tibetan Plateau. *J. Geophys. Res. Biogeosci.* **126**, e2020JG005951 (2021).
- Kirillin, G. B., Shatwell, T. & Wen, L. Ice-covered Lakes of Tibetan Plateau as solar heat collectors. *Geophys. Res. Lett.* **48**, e2021GL093429 (2021).
- Wang, Y. J., Shen, X. J., Jiang, M., Tong, S. Z. & Lu, X. G. Spatiotemporal change of aboveground biomass and its response to climate change in marshes of the Tibetan Plateau. *Int. J. Appl. Earth Observ. Geoinf.* **102**, 102385 (2021).
- Kouwenberg, L. L. R., Kurschner, W. M. & McElwain, J. C. Stomatal frequency change over altitudinal gradients: prospects for paleoaltimetry. *Rev. Mineral. Geochem.* **66**, 215–241 (2007).
- Wang, R. L. et al. Latitudinal variation of leaf stomatal traits from species to community level in forests: linkage with ecosystem productivity. *Sci. Rep.* **5**, 14454 (2015).
- Wu, B. F. et al. Land cover changes of China from 2000 to 2010. *Quaternary Sci.* **34**, 723–731 (2014).
- Kabacoff, R. R. *R in Action: Data Analysis and Graphics with R* (Manning Publications Co., 2015).
- Zhao, W. Z. et al. Variation and adaptation in leaf sulfur content across China. *J. Plant Ecol.* **15**, 743–755 (2022a).
- Ding, L. et al. Spatial patterns and driving factors of aboveground and belowground biomass over the eastern Eurasian steppe. *Sci. Total Environ.* **803**, 149700 (2022).
- Zhao, N. et al. Conservative allocation strategy of multiple nutrients among major plant organs: from species to community. *J. Ecol.* **108**, 267–278 (2019).
- Zhao, W. Z. et al. Spatial variation and allocation of sulfur among major plant organs in China. *Sci. Total Environ.* **844**, 157155 (2022b).
- Han, W. X., Fang, J. Y., Reich, P. B., Ian Woodward, F. & Wang, Z. H. Biogeography and variability of eleven mineral elements in plant leaves across gradients of climate, soil and plant functional type in China. *Ecol. Lett.* **14**, 788–796 (2011).
- Cheng, C. J. et al. Plant species richness on the Tibetan Plateau: patterns and determinants. *Ecography* **2023**, e06265 (2022).
- Hanum, C., Rauf, A., Fazrin, D. A. & Habibi, A. R. Nitrogen, phosphorus, and potassium level in soil and oil palm tree at various composition of plant species mixtures grown. *Earth Environ. Sci.* **41**, 012008 (2016).
- Pettersson, S. & Jensen, P. Variation among species and varieties in uptake and utilization of potassium. *Plant Soil* **72**, 231–237 (1983).
- Chen, G. S. et al. Allometry of fine roots in forest ecosystems. *Ecol. Lett.* **22**, 322–331 (2019).
- Ma, H. Z. et al. The global distribution and environmental drivers of aboveground versus belowground plant biomass. *Nat. Ecol. Evol.* **5**, 1110–1122 (2021).
- Zahoor, R. et al. Potassium fertilizer improves drought stress alleviation potential in cotton by enhancing photosynthesis and carbohydrate metabolism. *Environ. Exp. Botany* **137**, 73–83 (2017).
- Saadati, S., Baninasab, B., Mobli, M. & Gholami, M. Foliar application of potassium to improve the freezing tolerance of olive leaves by increasing some

- osmolite compounds and antioxidant activity. *Sci. Horticu.* **276**, 109765 (2021).
49. Poorter, H. & Nagel, O. The role of biomass allocation in the growth response of plants to different levels of light, CO₂, nutrients and water: a quantitative review. *Australian J. Plant Physiol.* **27**, 595–607 (2000).
50. Meng, F. C., Su, F. G., Li, Y. & Tong, K. Changes in terrestrial water storage during 2003–2014 and possible causes in Tibetan Plateau. *J. Geophys. Res. Atmos.* **124**, 2909–2931 (2019).
51. Tian, L. M. et al. Soil moisture and texture primarily control the soil nutrient stoichiometry across the Tibetan grassland. *Sci. Total Environ.* **622–623**, 192–202 (2018).
52. Sardans, J. & Penuelas, J. Potassium control of plant functions: ecological and agricultural implications. *Plants* **10**, 419 (2021).
53. Elser, J. J. et al. Growth rate-stoichiometry couplings in diverse biota. *Ecol. Lett.* **6**, 936–943 (2003).
54. Liu, C. C. et al. Relative effects of phylogeny, biological characters and environments on leaf traits in shrub biomes across central Inner Mongolia, China. *J. Plant Ecol.* **6**, 220–231 (2013).
55. Mederski, H. J. & Wilson, J. H. Relation of soil moisture to ion absorption by corn plants. *Soil Sci. Soc. Am. J.* **24**, 149–152 (1960).
56. Zhao, N. et al. Coordinated pattern of multi-element variability in leaves and roots across Chinese forest biomes. *Glob. Ecol. Biogeogr.* **25**, 359–367 (2016).
57. Sigdel, S. R. et al. Functional traits of a plant species fingerprint ecosystem productivity along broad elevational gradients in the Himalayas. *Functional Ecology* **37**, 383–394 (2023).
58. DeGroot, M. H. & Schervish, M. J. *Probability and Statistics*, 4th Edition. (Addison-Wesley, 2011).
59. Coussement, K. & Poel, D. V. D. Improving customer attrition prediction by integrating emotions from client/company interaction emails and evaluating multiple classifiers. *Expert Syst. Appl.* **36**, 6127–6134 (2009).

Acknowledgements

This work was supported by the National Natural Science Foundation of China (42141004, 31988102) and the Second Tibetan Plateau Scientific Expedition and Research Program (STEP, 2019QZKK060602). We are very grateful to all the teachers and students who helped us with the field survey and elemental measurement.

Author contributions

N.H. and M.L. designed the research. X.L., X.C., and L.X. conducted the fieldwork and collected the data. X.L. and N.H. led the writing of the manuscript. All authors contributed critically to the drafts and gave final approval for publication.

Competing interests

The authors declare no competing interests.

Additional information

Supplementary information The online version contains supplementary material available at <https://doi.org/10.1038/s43247-023-01033-8>.

Correspondence and requests for materials should be addressed to Mingxu Li or Nianpeng He.

Peer review information *Communications Earth and Environment* thanks Eryuan Liang and the other anonymous reviewer(s) for their contribution to the peer review of this work. Primary Handling Editor: Aliénor Lavergne. A peer review file is available.

Reprints and permission information is available at <http://www.nature.com/reprints>

Publisher's note Springer Nature remains neutral with regard to jurisdictional claims in published maps and institutional affiliations.



Open Access This article is licensed under a Creative Commons Attribution 4.0 International License, which permits use, sharing, adaptation, distribution and reproduction in any medium or format, as long as you give appropriate credit to the original author(s) and the source, provide a link to the Creative Commons licence, and indicate if changes were made. The images or other third party material in this article are included in the article's Creative Commons licence, unless indicated otherwise in a credit line to the material. If material is not included in the article's Creative Commons licence and your intended use is not permitted by statutory regulation or exceeds the permitted use, you will need to obtain permission directly from the copyright holder. To view a copy of this licence, visit <http://creativecommons.org/licenses/by/4.0/>.

© The Author(s) 2023